



Optically controlled coherent X-ray radiations from photo-excited nanotubes

Young-Min Shin *

Department of Physics, Northern Illinois University, DeKalb, IL 60115, USA

Accelerator Physics Center (APC), Fermi National Accelerator Laboratory (FNAL), Batavia, IL 60510, USA



ARTICLE INFO

Article history:

Received 19 June 2017

Received in revised form 21 July 2017

Accepted 22 July 2017

Keywords:

Betatron radiation

Carbon nanotube

X-ray

Coherent source

ABSTRACT

Relativistic electrons propagating through a plasmonic medium such as photo-excited plasma channels with negative permittivities undergo betatron motions, emitting photons at oscillating resonance modes. The similar betatron radiation can be generated in X-ray regimes from electrons transported through optically pumped carbon nanotubes (CNTs). The X-ray radiation condition of 0.5 and 6 MeV electrons phase-matched with plasmonic waves in CNTs is analyzed with a theoretical model of the CNT dispersion relation. Based on the dispersion analysis, radiation intensities and the brilliance of the coherent X-ray source averaged over the pulse duration are estimated using a typical range of system parameters of conventional electron sources and tabletop femtosecond lasers. The assessment indicates that the average brilliance of the harmonic radiation can reach 10^{10} – 10^{13} photons/s/mm²/mrad²/0.1%BW with 0.5–6 MeV electrons and X-ray energy up to a few keV.

© 2017 Elsevier B.V. All rights reserved.

1. Introduction

Light sources are one of the key tools for modern science and technology: they play a crucial role in a wide range of applications such as material processing/analysis [1] and lithography [2] in industry, imaging diagnosis [3] and radiological treatment [4] in bio-medicine, and noninvasive/nondestructive inspections [5] in defense and security. Such applications require photon sources with a large degree of spatiotemporal coherence. A significant increase of the brilliance and areal density will enable phase-contrast optical processing, X-ray fluorescence, X-ray diffraction/scattering, infrared FTIR-spectroscopy, and X-ray spectroscopy [6]. Laser-based radiation sources or laser-accelerators typically take advantage of intense driving lasers with extremely high power at the level of Terawatts or even Petawatts [7]. Such femtosecond laser systems occupy a large physical space, while the acceleration medium/target itself is much smaller than the driving source. Normally, a gas-jet is used for the laser-driven sources, but the laser-matter interaction in gas plasmas is unstable and has an intrinsically large energy spread. Laser interaction with a solid target is more stable and it offers exceptionally large EM fields: the field amplitude of photon-excited wakes in a plasma is increased with a plasma density, $E = m_e c \omega_p / e \approx 96 \times n_0^{1/2}$ [V/m], where

$\omega_p = (4\pi n_p e^2 / m_e)^{1/2}$ is the electron plasma frequency and n_p is the ambient plasma density of [electrons/cm³], m_e and e are the electron mass and charge, respectively, and c is the speed of light in vacuum. Crystals have several orders of magnitude higher density than gas plasmas [8]. However, crystal-targets become vulnerable to an intense laser and they are readily destroyed under the impact of a short pulse driving source. In theory, crystals are destroyed at a power density of 10^{12} W/cm² for nanosecond-long pulses (more practically, destruction would appear at 10^{13} – 10^{14} W/cm²) [9]. An accurate dissociation point of the crystal under a given energy density depends on the relaxation time to convert plasmon energy to phonons, but the required power densities seem to exceed the crystal fracture thresholds. Keeping the laser intensity sufficiently low, preferably below the target ionization threshold, would be more practical for the laser-based source application, especially for a compact system. Obviously, the lower laser intensities would be more compatible with a smaller system size. On the other hand, the reduction of radiation brilliance can be compensated by increasing laser-target coupling efficiency and/or pulse repetition rate instead. For such radiation based on a lower-power laser, structuring a solid target can be a benefit with improved electron-acceptance and laser coupling efficiency together with an increase of field confinements in the radiation region.

Carbon nanotubes are synthetic nanostructures consisting of honeycomb unit cells based on *sp*-2 carbon-bonding. CNTs can be a semiconductor or a metal depending on their chirality. In general,

* Address: Department of Physics, Northern Illinois University, DeKalb, IL 60115, USA.

E-mail address: yshin@niu.edu

armchair tubes are always metallic, while others can be semiconducting or metallic. Metallic CNTs are well suited for the laser-based radiation sources since oscillatory plasma waves can be readily generated by a photo-excitation in such metallic CNTs due to their negative permittivity [10]. If the optical wavelength of the driving laser is close enough to a plasma wavelength of a CNT, the laser would strongly perturb a density state of conduction electrons in atoms on the tube walls and excite surface plasmon polaritons (SPPs) [11]. The optical properties of CNT-SPP modes can be efficiently controlled by adjusting the tube parameters such as the diameter and tube-aerial density [12]. This paper presents the concept of laser-driven surface plasmon (SP) radiation in a carbon nanotube (CNT). An analytic description of the SP-assisted laser-pumped radiation will be detailed with practical system parameters, in particular with the specifications of a typical tabletop femtosecond laser system. Parametric relations of the plasmon-stimulated emissions utilizing optical properties of nanotubes will be analytically characterized.

2. Conceptual description with dispersion relations

When CNT-SPPs are excited by a laser, a photon-plasmon coupling condition is determined by the homogenized optical parameters of the porous substrate, e.g. plasma frequencies and refractive indices that are averaged over an area the size of the laser wavelength. The radiation mechanism of the laser-excited subwavelength plasmon is conceptually illustrated in Fig. 1. Metallic CNTs are effectively equivalent to hollow plasma channels. In such plasma channels, a plasma wake, if excited by a laser, would create harmonic EM waves [13–15] confined in the channel, which are analogous to plasmons in a CNT. A laser irradiated on a CNT-target modulates the electron density in a conduction band and quickly sets up a plasma oscillation at a laser-coupling condition. In other words, a laser can induce plasmons in a CNT as if plasma wakes excite the confined EM waves in a hollow plasma channel. The photo-excited density fluctuation induces evanescent EM waves that penetrate in the tube within the attenuation length [16]. The electrons with the kinetic energy (E_b) within a critical angle ($\theta_c = (2eV_0/E_b)^{1/2}$) of a CNT wall potential (V_0) or with divergences smaller than a CNT-geometrical acceptance would be transported in the nanotube. While moving along the tube, the electrons have betatron motions induced by a sinusoidally varying transverse field of the laser-excited plasmons [17]. The betatron oscillations will give rise to coherent radiations with harmonic components. The electron-plasmon synchronization remains until the electrons begin to outrun the confined field and become dephased from the plasmonic wave. A proper target thickness is

thus mainly determined by the dephasing length. Radiation parameters of subwavelength nanotubes are outlined in the following with more detailed specifications for a suitable femtosecond laser. Arrayed nanotubes have been analyzed with theoretical and numerical methods. For a given condition, a nanotube array can be described by a homogenized model with effective dielectric parameters: a nanotube can be treated as a superposition of overlapping cylinders of free electrons and immobile ions.

The dispersion/absorption relation of the periodic array [18] is given by

$$\kappa = k_r + ik_i \quad (1)$$

$$k_r(\omega) = \frac{\omega}{c} \sqrt{\frac{\left(\epsilon_L - \frac{\omega_p^2}{\omega^2 - \omega_p^2/2}\right) \left(\epsilon_L - \frac{\omega_p^2}{\omega^2 - \omega_p^2}\right)}{\epsilon_L - \left(\omega_p^2/\omega^2 - \omega_p^2\right) \left(\cos^2 \theta + \frac{\omega^2}{\omega^2 - \omega_p^2/2} \sin^2 \theta\right)}} \quad (2)$$

$$k_i(\omega) = \frac{\omega^3 v \omega_p^2}{2c^2 (\omega^2 - \omega_p^2)^2 k_r} \times \left(\frac{\epsilon_L - \frac{\omega_p^2}{\omega^2 - \omega_p^2/2} + \left(\epsilon_L - \frac{\omega_p^2}{\omega^2 - \omega_p^2}\right) \left(\frac{\omega^2 - \omega_p^2}{(\omega^2 - \omega_p^2/2)^2}\right)}{\epsilon_L - \frac{\omega_p^2}{\omega^2 - \omega_p^2} \left(\cos^2 \theta + \frac{\omega^2 - \omega_p^2}{\omega^2 - \omega_p^2/2} \sin^2 \theta\right)} - \frac{\left(\epsilon_L - \frac{\omega_p^2}{\omega^2 - \omega_p^2/2}\right) \left(\epsilon_L - \frac{\omega_p^2}{\omega^2 - \omega_p^2}\right) + \left(\cos^2 \theta + \frac{\omega^2 - \omega_p^2}{(\omega^2 - \omega_p^2/2)^2} \sin^2 \theta\right)}{\left(\epsilon_L - \frac{\omega_p^2}{\omega^2 - \omega_p^2} \left(\cos^2 \theta + \frac{\omega^2 - \omega_p^2}{\omega^2 - \omega_p^2/2} \sin^2 \theta\right)\right)^2} \right) \quad (3)$$

Here, $\omega_p = \sqrt{\frac{n_e e^2}{\epsilon_0 m}}$, $n_e = Zn_0$, and $\omega_p^2 = s\omega_p^2$ (n_0 is the ion density of a single CNT and $s = \pi r_t^2/d^2$ is the aerial CNT-filling ratio). Taking advantage of the homogenized dielectric model [19], the dispersion/absorption relations of a CNT-confined SPP are analyzed with respect to a p-polarized laser, as plotted in Fig. 2(a) and (b) ($n_e = 10^{21} \text{ cm}^{-3}$, r_c (tube radius) = 50 nm, and $d = N_c^{-1/2}$ (separation between tubes) = 150 nm, $\pi r_c^2 N_c \sim 0.35$, $v/\omega_p \sim 0.001$, and areal density N_c). Here, $\omega_p = \sqrt{n_e e^2/\epsilon_0 m}$, $n_e = Zn_0$, and $\omega_p^2 = s\omega_p^2$ (n_0 is the ion density of a single CNT, $s = \pi r_t^2/d^2$ is the aerial CNT-filling ratio, and Z is the atomic number). Given that a single CNT is sized from a few tens of nanometers up to 1 μm in diameter, which is the equivalent of a few hundred nanometers to a few microns of unit area on a target, the effective electron plasma density averaged over a volume of the CNT ranges from 10^{21} – $10^{23} \text{ e}^-/\text{cm}^3$. Under the resonance condition, the laser is

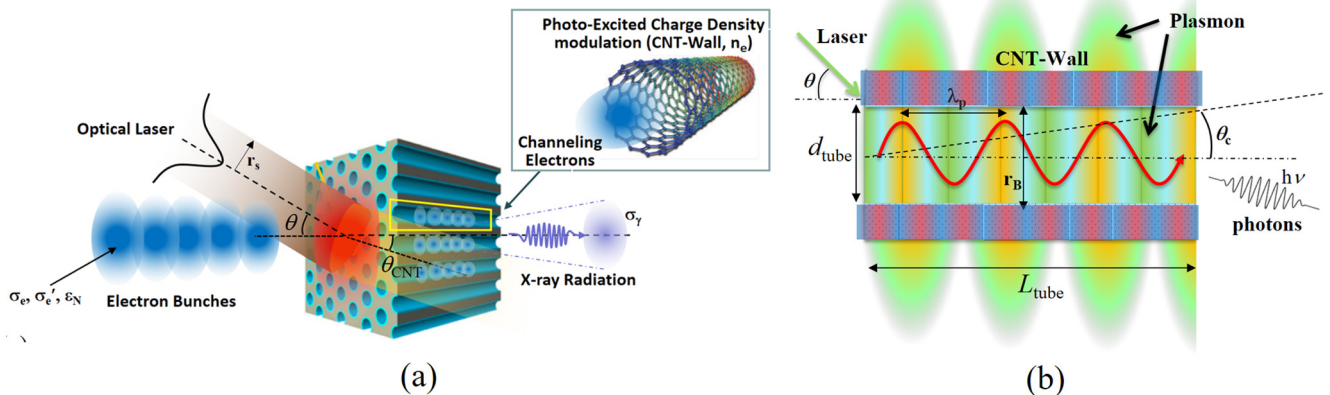


Fig. 1. Conceptual drawings of (a) optically pumped nanotube (b) X-ray radiation of photo-excited CNT.

Download English Version:

<https://daneshyari.com/en/article/5467539>

Download Persian Version:

<https://daneshyari.com/article/5467539>

[Daneshyari.com](https://daneshyari.com)